ECS Journal of Solid State Science and Technology, 2022 **11** 101009
2162-8777/2022/11(10)/101009/6/$40.00 © 2022 The Electrochemical Society ("ECS"). Published on behalf of ECS by IOP Publishing Limited

Optimization of ssDNA-SWCNT Ultracentrifugation via Efficacy Measurements

Zachary Cohen,[1] Sadiyah Parveen,[1] and Ryan M. Williams[1,2,z]

[1]*The City College of New York, Department of Biomedical Engineering, New York, NY 10031, United States of America*
[2]*PhD Program in Chemistry, Graduate Center, City University of New York, New York, NY 10016, United States of America*

Photoluminescent single-walled carbon nanotubes (SWCNT) hold substantial potential for a variety of applications in biology and medicine. Improved preparation of such materials requires optimization of various parameters, including those pertaining to ultracentrifugation techniques for removing non-photoluminescent carbonaceous materials. In this work, we investigated single-stranded DNA (ssDNA)-SWCNT preparations, which are widely used and exhibit strong photoluminescence (PL). We found, however, that total PL is not well-described by SWCNT concentration, and that it is much more sufficiently described by a comparison of SWCNT E_{22} transition peaks with surrounding baseline absorbance from non-fluorescent carbonaceous material. We used this metric, defined as efficacy, in optimizing techniques for centrifugation and subsequent fractionation. We found that increased centrifugal forces removed substantial non-photoluminescent material, but also more SWCNT mass, yielding less-concentrated but more-pure fluorescent SWCNT samples. Thus, a tradeoff exists between decreased sensor material and increased sensor quality, one which might be considered for each novel SWCNT-based nanosensor construct. We anticipate these studies serving as a basis for improved applied nanosensor development.
 [DOI: 10.1149/2162-8777/ac9929]

Manuscript submitted August 17, 2022; revised manuscript received September 25, 2022. Published October 19, 2022. *This paper is part of the JSS Focus Issue on ECS Nano: Early Career Researchers.*

Single-walled carbon nanotubes (SWCNT) are quasi-one-dimensional cylindrical fullerenes[1] which hold tremendous potential in a variety of applications, including biological and chemical sensing, drug delivery, green energy, additive manufacturing, electronics, and others.[2,3] Sensors featuring SWNCT as signal transducers, or as components of the recognition element itself, often rely on their electrochemical or photoluminescence (PL) properties, which have been increasingly utilized in research and development over the past several decades.[4,5] These multitudinous uses have increased fundamental interest in optimization of SWCNT preparation.

As biological or chemical sensors, SWCNT exhibit several ideal optical properties.[6–8] Their PL emission lies in the near-infrared range, therefore allowing penetration of several centimeters through tissue and other biological media.[9] SWCNT are also highly photostable, allowing for continuous, long-term interrogation.[4] Importantly, SWCNT PL is modulated by the local environment, allowing for surface engineering to create specific sensor devices.[4] Such advantages have led to the development of highly-specific sensors for surface-based,[10–14] in vitro,[15] intra-[16] and -extra-cellular[17] and even in vivo use.[11,18–21] Examples include sensors for small molecules such as dopamine[13] or chemotherapeutics,[22,23] nucleic acids,[19] cell surface environments,[17] protein biomarkers,[24] and others.[25]

Owing to their surface composition, as-prepared SWCNT are highly hydrophobic and do not suspend in aqueous solutions.[2] Approaches to obtain stable SWCNT dispersions include encapsulation by bile salt surfactants,[26] polymers,[27] lipids,[28] peptides,[29] and nucleic acids.[30] Of these, nucleic acids have been the most widely studied for several reasons, including pi-pi stacking of bases on the carbon surface,[30] sequence selectivity for various chiralities,[30] chemical modifiers for site-directed conjugations,[31] and long-term biocompatibility and stability.[32] Further, the interaction of single-stranded DNA (ssDNA) with SWCNT is well-characterized and has even served as the basis for biomarker-specific molecular recognition.[33–35]

Suspensions of ssDNA-SWCNT are typically prepared by focused probe-tip ultrasonication to break up and disperse SWCNT bundles, allowing pi-pi stacking with ssDNA.[36] This preparation is then typically ultracentrifuged at high speed to remove undispersed carbonaceous material.[11] The resultant ssDNA-SWCNT suspension is then filtered to remove remaining ssDNA just prior to use.[11] However, inefficiencies in this process, whether during sonication or ultracentrifugation, reduce the mass and/or PL yield of prepared sensor.[37] Measurements of SWCNT quantum yield are somewhat variable, and those of suspensions prepared as described above are affected by energy absorption from non-photoluminescent material (bundled SWCNT or amorphous carbon).[36,37] Thus, we sought to optimize removal of such material through ultracentrifugation. To do so, we defined a metric, efficacy, as a proxy measurement of a ssDNA-SWCNT sample's purity. It seeks to measure the fraction of light at the excitation wavelength which is absorbed by E_{22} transitions compared to that absorbed by non-fluorescent carbonaceous material. This metric is similar to prior approaches that sought to determine background contributions to SWCNT E_{22} transition measurements,[36–39] a concept previously termed "resonance ratio".[38]

Experimental

Standard ssDNA-SWCNT preparation.—Suspensions of ssDNA and SWCNT were prepared for photoluminescence measurements as previously described.[11,15,19,22] Briefly, 1 mg $(GT)_{15}$ ssDNA (Integrated DNA Technologies; Coralville, IA) were added to 0.5 mg HiPCO SWCNT (NanoIntegris; Boisbriand, Canada) in 0.5 ml 1X phosphate buffered saline (PBS). Samples were sonicated at 40% amplitude by a 120 W ultrasonicator with 1/8″ probe microtip (Fisher Scientific; Hampton, NH) while on ice for one hour. The preparation was ultracentrifuged at 230,000 X g within 4 ml polycarbonate centrifuge tubes (Beckman Coulter; Brea, CA) for 30 min in an Optima Max-XP Ultracentrifuge (Beckman Coulter) fit with a MLA-50 rotor. Typically, the top 75% of the supernatant was recovered and subjected to 100 kDa Amicon Ultra 0.5 ml centrifugal filters (Sigma-Aldrich; St. Louis, MO) for 15 min at 14,000 X g. The portion of solution retained above the filter, containing ssDNA-SWCNT, was washed once with 200 μl 1X PBS and centrifuged again. The top was again recovered by resuspension with the same volume of 1X PBS and subjected to further analysis. A total of 63 such ssDNA-SWCNT preparations were initially analyzed to determine the correlation between their absorbance and fluorescence output.

UV–vis absorbance and concentration measurement.—Samples of ssDNA-SWCNT recovered after filtration were subjected to absorbance measurements from 300–1100 nm using a V-730 UV–vis Spectrophotometer (Jasco; Easton, MD) with a 400 nm min^{-1} scan rate and 0.2 nm steps. Recovered samples were diluted 100-fold (or greater, if necessary to obtain $A_{630} < 0.5$) with 1X PBS

[z]E-mail: rwilliams4@ccny.cuny.edu

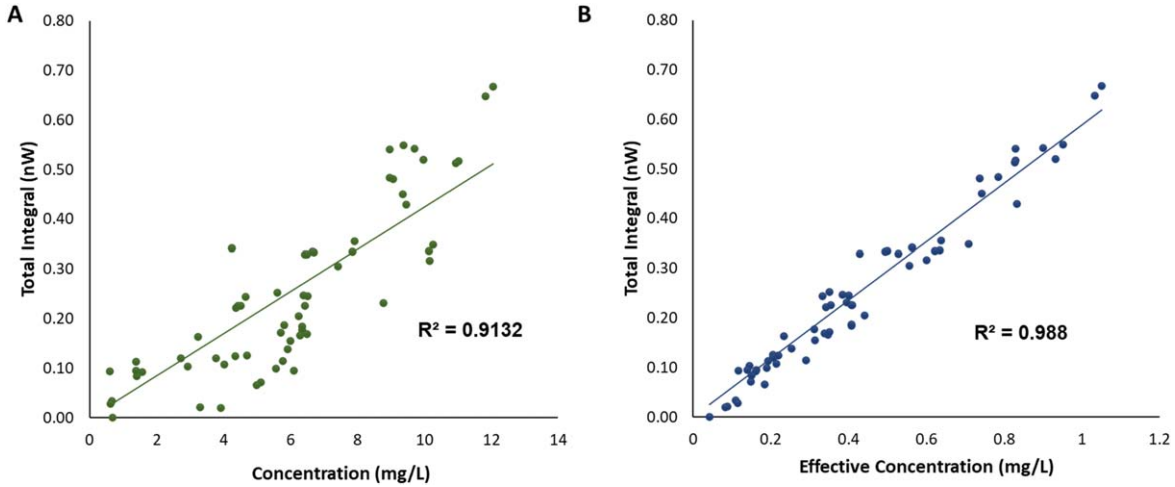

Figure 1. Total fluorescence integral as a function of concentration or effective concentration. (A) Total fluorescence integral of a ssDNA-SWCNT preparation was plotted vs the measured concentration determined by absorbance spectroscopy. (B) The same plotted against effective concentration.

prior to measurement. As previously determined,[5,10,19,29] the concentration of SWCNT was evaluated using the absorbance at the valley near 630 nm using the equation: $C = A_{630}/0.036\ l\ mg^{-1}\ cm^{-1} * D$, wherein C = concentration of SWCNT; A_{630} = value of the absorbance minimum near 630 nm; and D = dilution factor.

Near-Infrared fluorescence emission.—Photoluminescence of ssDNA-SWCNT samples was obtained in the range of 900–1600 nm using a NS MiniTracer (Applied NanoFluorescence; Houston TX). Samples were diluted 100X in 1X PBS and measured in a plastic microcuvette (BrandTech; Essex, CT) by excitation with a 110 mW 638 nm laser. Total fluorescence integral was determined for each sample by instrument software.

Optimizing ultracentrifugation parameters.—$(GT)_{15}$ ssDNA—HiPCO SWCNT were prepared via ultrasonication as above. In triplicate, a total of five 500 μl batches were prepared via ultrasonication as above and combined for homogeneity (three separate combined preparations were prepared and analyzed individually). The combined suspensions were then divided into five aliquots of 500 μl each. One was not centrifuged, while one aliquot each was centrifuged at 14,000, 29,000, 58,000, or 115,000 X g each. As above, the upper 75% of the supernatant was collected from ultracentrifuged samples. However, in this experiment, the lower 25% (excluding the pellet) was also collected for analysis. SWCNT pools and supernatant fractions were optically characterized as above.

Evaluation of efficacy and effective mass.—Each fraction (upper 75% and lower 25%) of each sample was analyzed to determine the SWCNT concentration, recovered mass, fluorescence efficacy, and the effective mass.

Mass (M) was calculated as: M = C * TV, wherein M = mass; C = concentration determined as above; and TV = total volume recovered.

Efficacy (E) was determined to be: $E = (A_{655}—A_{630})/A_{655}$. This measurement describes the proportion of light that is absorbed by dispersed SWCNT in a sample and leads to observed fluorescence. In principle, this metric can be adapted for other work by selecting alternative absorbance maxima and adjacent minima. The absorbance maximum near 655 nm was selected because it corresponds to SWCNT excited by the 638 nm laser used for probing, predominantly the (7,5) and (7,6) chiralities.

Effective Concentration (EC) was determined to be: EC = E * C, whereas Effective Mass (EM) was determined to be: EM = E * M. These metrics (EC and EM), which correlate with a given SWCNT sample's expected PL intensity, were plotted as function of centrifugal force.

Sample efficacy and mass were fit with logistic models: f(x) = a + [(bx)/(c+x)]. The effective mass model was the product of the efficacy and mass models.

Results

Evaluation of total fluorescence as a function of SWCNT mass or effective concentration.—Initial studies which motivated these experiments evaluated the total PL emission from as-prepared $(GT)_{15}$ ssDNA—HiPCO SWCNT samples as a function of their concentration in solution. These studies found that substantial heterogeneity existed between samples, evidenced by an R^2 of 0.91 over 63 samples (Fig. 1a). Due to this lack of sound correlation, we sought to define an alternate metric to determine the overall quality of ssDNA-SWCNT preparation.

In doing so, we determined the efficacy and effective concentration (EC) for each sample. Efficacy is the percentage of absorption near the excitation wavelength (in this case 638 nm) attributable to SWCNT E_{22} transitions; effective concentration is the product of efficacy and concentration. The same 63 samples were evaluated, finding a very strong, positive association between their effective concentrations and PL intensities, with an R^2 of 0.99 (Fig. 1b). Thus, we concluded that efficacy was a suitable proxy for SWCNT sample quality, as it accounts for differences in sample PL intensity not explained by comparison of their concentrations alone.

Evaluation of centrifugal force on SWCNT recovery and efficacy.—We sought to determine the effect of modifying centrifugal force on ssDNA-SWCNT preparations by evaluating the total effective mass (EM) of each. In triplicate, large batches of prepared ssDNA-SWCNT were split into aliquots which were centrifuged at 14,000, 29,000, 58,000, and 115,000 X g (Table I). Absorbance spectra were obtained from 300–1100 nm for both the top 75% and bottom 25% of the supernatant fractions separately (Fig. 2). In this work, however, we modeled the effects of varying centrifuge force on a sample's supernatant as a whole (top and bottom fractions combined). The large stock batches were similarly characterized without centrifugation for comparison. The SWCNT masses in 500 μl of these stocks were calculated for comparison.

As expected, the mass of recovered SWCNT decreased with increased centrifugal force (Fig. 3a). At centrifugal speeds of 14,000 X g, approximately 20% of the total mass was removed compared to the uncentrifuged stock, whereas 58% of the mass was removed at 115,000 X g. Interestingly, this removal of additional mass led to an

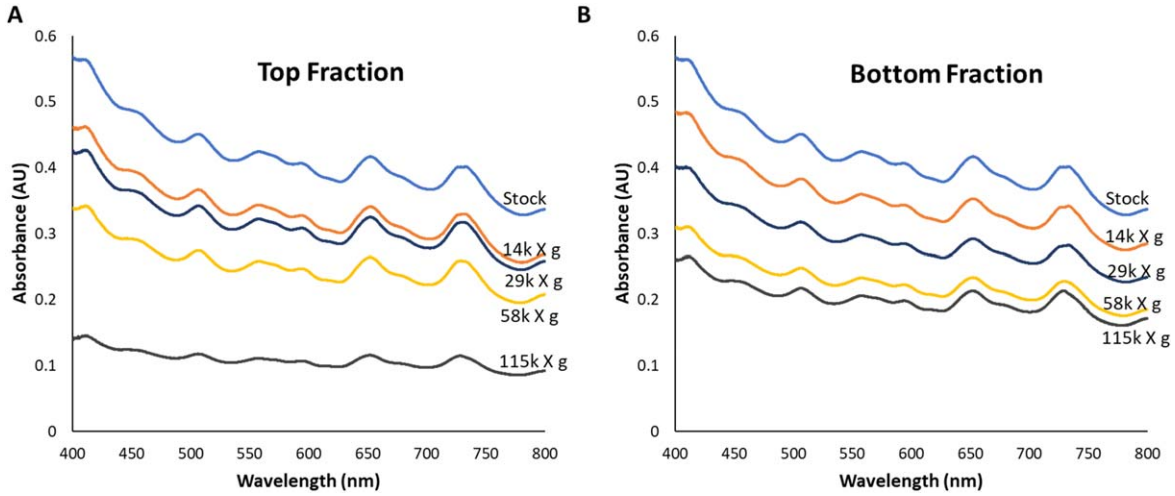

Figure 2. Absorbance spectra obtained from ultracentrifuged SWCNT supernatants. (A) Representative absorbance spectra obtained from the top 75% fraction of ssDNA-SWCNT subjected to no centrifugation (stock) or centrifugation at the given speeds (14 k X g = 14,000 X g). (B) Bottom 25% fraction of the same. Note that various dilution factors were used and thus these spectra do not reflect concentration directly.

Table I. Effect of centrifugal force on SWCNT efficacy.

Centrifugal Force (k X g)	Mass (μg)	±	Efficacy (%)	±	Effective Mass (μg)	±
0	487.0	51.4	9.0	0.9	42.3	5.1
14	391.5	35.3	10.6	1.0	41.6	5.1
29	336.2	49.3	11.6	1.4	38.8	5.7
58	268.8	40.7	13.3	1.5	35.6	5.1
115	177.7	31.3	15.3	4.3	27.2	4.0

increase in efficacy (E), from approximately 9% in the uncentrifuged stock, to just 11% with the lowest centrifugal force, to over 15% with the highest centrifugal force, an increase of approximately 60% from the stock (Table I; Fig. 3b). These outcomes led to similar effective masses in samples centrifuged at the lowest force vs an equivalent volume of the uncentrifuged stock (42.3 vs 41.6 μg in 500 μl), with a substantial drop-off of over 30% from 58,000 to 115,000 X g (Table I; Fig. 3c).

Investigating top vs bottom fractions of ssDNA-SWCNT sample supernatant.—We next investigated the necessity of removing the top 75% of recovered ssDNA-SWCNT samples, which is standard practice to ensure removal of SWCNT bundles not in the pellet (Table II). As expected for the lowest three centrifugal speeds, the top fraction mass was approximately 3-fold greater than the bottom fraction mass (Table I; Fig. 4a), whereas the masses were approximately similar for the 115,000 X g force. In all cases, the efficacy (E) was greater for the top fraction than the bottom fraction, ranging from 6.8–33.3% greater, with the smallest differences being at 115,000 X g (Fig. 4b). Both top and bottom fractions of samples centrifuged at this force exhibited significant improvement compared to the uncentrifuged stock, with efficacy increases >66% (stock = 8.9%, top = 15.8%, bottom = 14.8%).

Discussion

In this work, we investigated parameters for ultracentrifugation to optimize removal of non-photoluminescent carbon material in the preparation of ssDNA-SWCNT. These studies were motivated by our observation that total PL of SWCNT samples was not well-described by their measured concentrations, and the necessity of improving the ssDNA-SWCNT preparation process. Therefore, we developed metrics of efficacy, effective concentration, and effective mass, which allowed us to quickly and easily assess SWCNT sample quality by approximating the proportion of SWCNT to non-fluorescent carbonaceous material. These metrics are similar to prior approaches in the field which compared the contributions of background impurities to absorbance of E_{22} transitions.[36–39] We found these metrics to be much better predictors of a sample's total PL intensity.

Using these metrics, we systematically evaluated proper centrifugal conditions to remove background carbonaceous material. Standard practice is to use high-speed ultracentrifugation to remove this and other unwanted materials. Indeed, ultracentrifugation methodology for SWCNT preparation is well characterized, including methods of density gradient separation and surfactant-induced purification.[40–42] We investigated centrifugal speeds in two-fold increments from 14,000 X g to 115,000 X g and compared those to uncentrifuged stock ssDNA-SWCNT sonicated preparations. As expected, maximal centrifugal speeds removed up to 58% of the mass from the samples, whereas substantially smaller amounts were removed by lighter centrifugation (20%). This achieved improved sample quality, with increasing centrifugal speeds leading to monotonic increases in sample efficacy up to 78%. However, this inevitably led to decreases in the effective mass of SWCNT; although there was substantially less background absorbance, there was also substantially less dispersed SWCNT material.

Finally, we evaluated the common practice of only using the upper portion (~75%) of the centrifugal supernatant. We found that, as expected, the upper portion had greater efficacy than the lower. This difference was substantial (up to 33.3% more) at lower centrifugal speeds, though less substantial (just 6.8%) at the maximal speed. The optimal centrifuge force for maximum dispersion quality was found to be 115,000 X g, as it led to the greatest efficacy increase vs the stock for top and bottom fractions. indicating that it removed the most non-fluorescent material. This conclusion is supported by the total mass removed.

This work is both important and nuanced in that it highlights the tradeoffs in nanosensor preparation. It is clear that no single ssDNA-SWCNT preparation protocol can be used in all situations. If the sensors are to be used in vivo, for example, it may be necessary to maximize total fluorescence of the samples by increasing their

Table II. Effect of fractionation on efficacy of centrifugal supernatant.

	Top			Bottom			Combined		
Centrifugal Force (k X g)	Mass (μg)	Efficacy (%)	Effective Mass (μg)	Mass (μg)	Efficacy (%)	Effective Mass (μg)	Mass (μg)	Efficacy (%)	Effective Mass (μg)
0	448.5	8.9	39.9						
±	87.7	0.93	6.4						
14	285.2	11.1	31.8	106.3	9.3	9.9	391.5	10.6	41.7
±	45.6	0.04	5.2	4.2	3.7	0.0	49.8	0.09	5.2
29	252.5	12.4	31.2	83.7	9.3	7.7	336.2	11.6	38.9
±	41.4	1	4.7	8.1	2.5	1.8	49.4	1.4	5.8
58	181.0	14.7	26.4	70.2	11.9	7.2	268.9	13.3	35.6
±	53.5	1.1	6.4	26.8	3.6	1.1	40.7	1.5	5.1
115	86.6	15.8	13.7	91.1	14.8	13.5	177.7	15.3	27.2
±	15.0	0.49	1.9	16.4	0.4	2.1	31.3	0.43	4.0

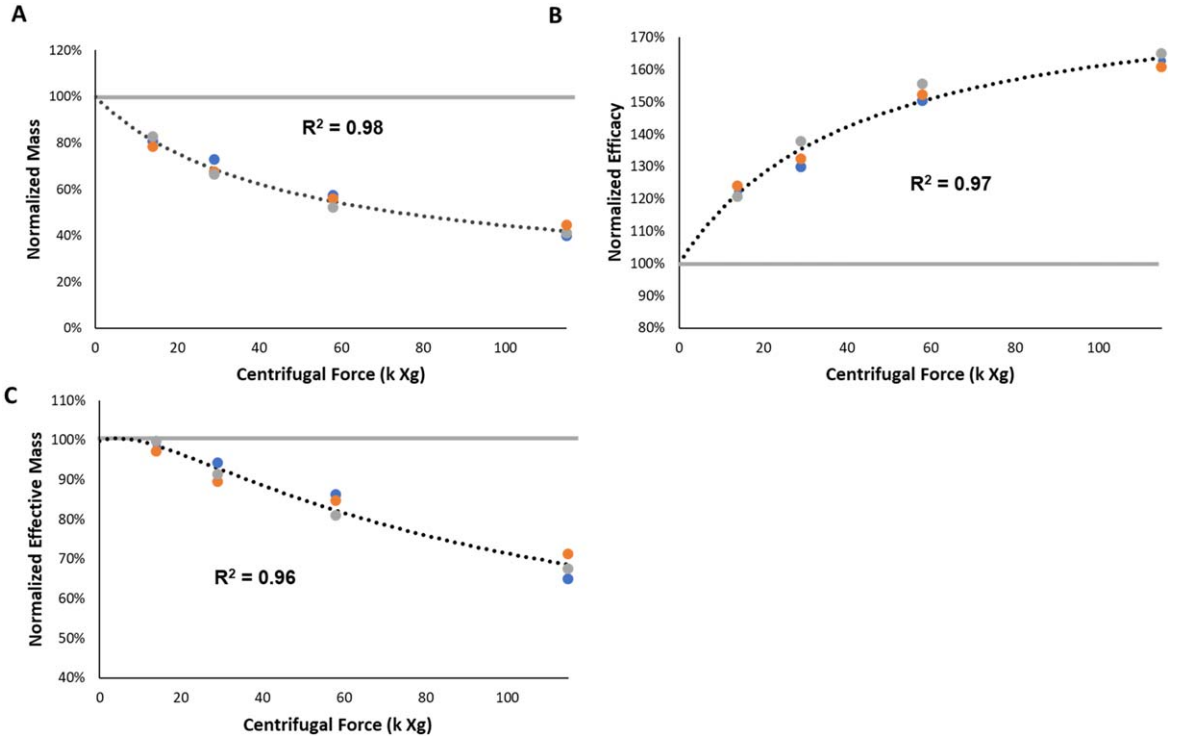

Figure 3. Combined analysis of ssDNA-SWCNT centrifugal speeds. The mass (A), efficacy (B), and effective mass (C) of recovered ssDNA-SWCNT from ultracentrifugal supernatants, plotted against centrifugal force. Series are represented by color of circles, with experiments performed in triplicate. Data are presented as a percentage of the data from the stock solution with no centrifugation performed, which is represented as 100%. Best-fit lines are logistic fits.

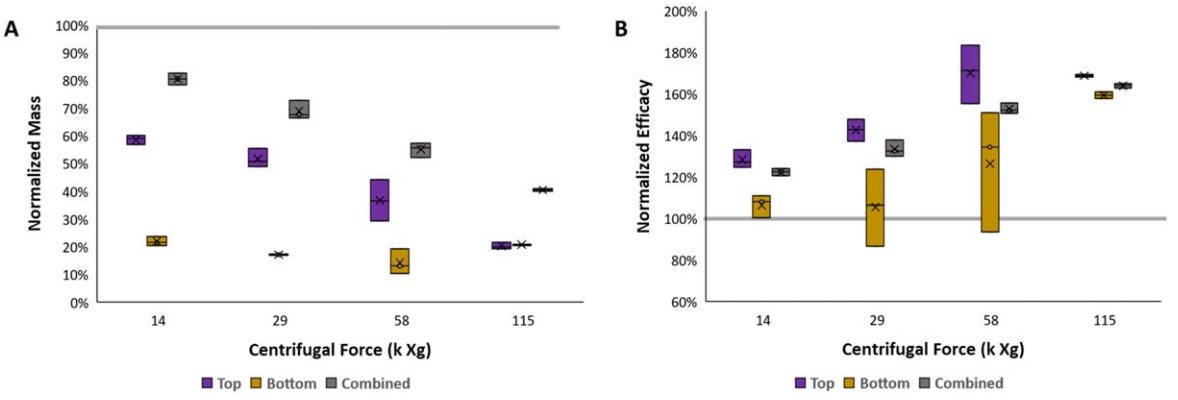

Figure 4. Analysis of top and bottom supernatant fractions. The mass (A) and efficacy (B) of the top 75% and bottom 25% fractions of ultracentrifugal supernatant for each centrifugal force investigated were plotted in comparison to the data of each fraction combined. Box plots show minimum, median, and maximum of triplicate data with mean represented by an "X". Data are presented as a percentage of the data from the stock solution with no centrifugation performed, which is represented as 100%.

efficacy (E_{22} absorbance above background) through increased centrifugal force.[14] However, in applications where larger quantities of SWCNT are necessary and brightness per amount of sample is not a concern, such as in nanosensor arrays or films for example, lower centrifugal forces around 58,000 X g may be sufficient.[10–14] We found that there are similar tradeoffs to be considered in discarding the bottom fraction of centrifugal supernatant. Thus, it is recommended that these studies may be followed as guidelines for each investigator in the preparation of their own sensor constructs.

These studies portend additional investigation into the optimization of photoluminescent SWCNT. In medicine and biology, SWCNT PL may serve useful for sensors or diagnostic tools.[43] However, it remains to be seen how alterations in centrifugal force may affect sensor response to various analytes, if at all. We also expect that results may vary based on how the SWCNT were synthesized, if other than HiPCO, or if they were enriched for specific chiralities. We do expect, however, that modification of this protocol would allow for better evaluation of chirality-enriched SWCNT preparations, whose concentrations may prove difficult to determine using standard extinction coefficients. Additionally, the effects of varying centrifugation duration were not investigated. Finally, it remains to be seen whether the optical properties of SWCNT dispersed by other, non-ssDNA surfactants are affected by centrifugation in the same manner, though it is expected that these guidelines are widely applicable.

Conclusions

In this work, we evaluated the effect of ultracentrifugation speed and fractionated supernatant recovery on the preparation of ssDNA-SWCNT for nanosensor constructs. To do so, we defined the metrics

of sample efficacy and effective mass, the former to approximate what proportion of a sample's absorbance is related to SWCNT E_{22} transitions and the latter as a predictor of a sample's total fluorescence. We expect these metrics may be more useful in estimating a SWCNT preparation's total amount of photoluminescent material than those derived from concentration alone. We also anticipate these studies will help guide preparation of SWCNT sensor constructs dependent upon the intended application.

Acknowledgments

The authors would like to acknowledge members of the Williams Lab for input and feedback on this work. This work was supported by a CUNY ASRC (City University of New York Advanced Science Research Center) Seed Award, a PSC-CUNY (Professional Staff Congress of CUNY) Enhanced Award, and The City College of New York Grove School of Engineering Department of Biomedical Engineering. SP was supported by the NSF CCNY Summer Research Fellowship Program (NSF Grant # 1832567).

ORCID

Ryan M. Williams https://orcid.org/0000-0002-2381-8732

References

1. S. Iijima, "Helical microtubules of graphitic carbon." *Nature*, **354**, 56 (1991).
2. M. S. Dresselhaus, G. Dresselhaus, P. Eklund, and A. Rao, *in The physics of fullerene-based and fullerene-related materials* 331 (Berlin)(Springer) (2000).
3. A. Jorio, G. Dresselhaus, and M. S. Dresselhaus, *Carbon nanotubes: Advanced Topics in the Synthesis, Structure, Properties and Applications* Vol. 111 (Berlin) (Springer) (2008).
4. A. A. Boghossian, J. Zhang, P. W. Barone, N. F. Reuel, J. H. Kim, D. A. Heller, J. H. Ahn, A. J. Hilmer, A. Rwei, and J. R. Arkalgud, "Near-infrared fluorescent sensors based on single-walled carbon nanotubes for life sciences applications." *Chem Sus Chem*, **4**, 848 (2011).
5. H. Beitollahi, F. Movahedifar, S. Tajik, and S. Jahani, "A review on the effects of introducing CNTs in the modification process of electrochemical sensors." *Electroanalysis*, **31**, 1195 (2019).
6. M. J. O'connell, S. M. Bachilo, C. B. Huffman, V. C. Moore, M. S. Strano, E. H. Haroz, K. L. Rialon, P. J. Boul, W. H. Noon, and C. Kittrell, "Band gap fluorescence from individual single-walled carbon nanotubes." *Science*, **297**, 593 (2002).
7. P. V. Jena, T. V. Galassi, D. Roxbury, and D. A. Heller, "Progress toward applications of carbon nanotube photoluminescence." *ECS J. Solid State Sci. Technol.*, **6**, M3075 (2017).
8. S. M. Bachilo, M. S. Strano, C. Kittrell, R. H. Hauge, R. E. Smalley, and R. B. Weisman, "Structure-assigned optical spectra of single-walled carbon nanotubes." *Science*, **298**, 2361 (2002).
9. K. Welsher, S. P. Sherlock, and H. Dai, "Deep-tissue anatomical imaging of mice using carbon nanotube fluorophores in the second near-infrared window." *Proc. Natl Acad. Sci.*, **108**, 8943 (2011).
10. S. Elizarova, A. A. Chouaib, A. Shaib, B. Hill, F. Mann, N. Brose, S. Kruss, and J. A. Daniel, "A fluorescent nanosensor paint detects dopamine release at axonal varicosities with high spatiotemporal resolution." *Proc. Natl Acad. Sci.*, **119**, e2202842119 (2022).
11. R. M. Williams, C. Lee, T. V. Galassi, J. D. Harvey, R. Leicher, M. Sirenko, M. A. Dorso, J. Shah, N. Olvera, and F. Dao, "Noninvasive ovarian cancer biomarker detection via an optical nanosensor implant." *Sci. Adv.*, **4**, eaaq1090 (2018).
12. M. M. Safaee, M. Gravely, and D. Roxbury, "A wearable optical microfibrous biomaterial with encapsulated nanosensors enables wireless monitoring of oxidative stress." *Adv. Funct. Mater.*, **31**, 2006254 (2021).
13. S. Kruss, D. P. Salem, L. Vuković, B. Lima, E. Vander Ende, E. S. Boyden, and M. S. Strano, "High-resolution imaging of cellular dopamine efflux using a fluorescent nanosensor array." *Proc. Natl Acad. Sci.*, **114**, 1789 (2017).
14. C. Bulumulla, A. T. Krasley, B. Cristofori-Armstrong, W. C. Valinsky, D. Walpita, D. Ackerman, D. E. Clapham, and A. G. Beyene, "Visualizing synaptic dopamine efflux with a 2D composite nanofilm." *Elife*, **11**, e78773 (2022).
15. R. M. Williams, C. Lee, and D. A. Heller, "A fluorescent carbon nanotube sensor detects the metastatic prostate cancer biomarker uPA." *ACS Sens.*, **3**, 1838 (2018).
16. P. V. Jena, D. Roxbury, T. V. Galassi, L. Akkari, C. P. Horoszko, D. B. Iaea, J. Budhathoki-Uprety, N. Pipalia, A. S. Haka, and J. D. Harvey, "A carbon nanotube optical reporter maps endolysosomal lipid flux." *ACS nano*, **11**, 10689 (2017).
17. D. Roxbury, P. V. Jena, Y. Shamay, C. P. Horoszko, and D. A. Heller, "Cell membrane proteins modulate the carbon nanotube optical bandgap via surface charge accumulation." *ACS nano*, **10**, 499 (2016).
18. N. M. Iverson et al., "In vivo biosensing via tissue-localizable near-infrared-fluorescent single-walled carbon nanotubes." *Nat. Nanotechnol.*, **8**, 873 (2013).
19. J. D. Harvey, P. V. Jena, H. A. Baker, G. H. Zerze, R. M. Williams, T. V. Galassi, D. Roxbury, J. Mittal, and D. A. Heller, "A carbon nanotube reporter of microRNA hybridization events in vivo." *Nat. Biomed. Eng.*, **1**, 0041 (2017).
20. E. Hofferber, J. Meier, N. Herrera, J. Stapleton, C. Calkins, and N. Iverson, "Detection of single walled carbon nanotube based sensors in a large mammal." *Nanomed. Nanotechnol. Biol. Med.*, **40**, 102489 (2022).
21. T. V. Galassi, P. V. Jena, J. Shah, G. Ao, E. Molitor, Y. Bram, A. Frankel, J. Park, J. Jessurun, and D. S. Ory, "An optical nanoreporter of endolysosomal lipid accumulation reveals enduring effects of diet on hepatic macrophages in vivo." *Sci. Transl. Med.*, **10**, eaar2680 (2018).
22. J. D. Harvey, R. M. Williams, K. M. Tully, H. A. Baker, Y. Shamay, and D. A. Heller, "An in Vivo nanosensor measures compartmental doxorubicin exposure." *Nano Lett.* (2019).
23. J. D. Harvey, H. A. Baker, E. Mercer, J. Budhathoki-Uprety, and D. A. Heller, "Control of carbon nanotube solvatochromic response to chemotherapeutic agents." *ACS Appl. Mater. Interfaces*, **9**, 37947 (2017).
24. A. Hendler-Neumark and G. Bisker, "Fluorescent single-walled carbon nanotubes for protein detection." *Sensors*, **19**, 5403 (2019).
25. J. Kupis-Rozmysłowicz, A. Antonucci, and A. A. Boghossian, "Engineering the Selectivity of the DNA-SWCNT Sensor." *ECS J. Solid State Sci. Technol.*, **5**, M3067 (2016).
26. J. K. Streit, J. A. Fagan, and M. Zheng, "A low energy route to DNA-wrapped carbon nanotubes via replacement of bile salt surfactants." *Anal. Chem.*, **89**, 10496 (2017).
27. J. Budhathoki-Uprety, P. V. Jena, D. Roxbury, and D. A. Heller, "Helical polycarbodiimide cloaking of carbon nanotubes enables inter-nanotube exciton energy transfer modulation." *J. Am. Chem. Soc.*, **136**, 15545 (2014).
28. R. Ehrlich, A. Hendler-Neumark, V. Wulf, D. Amir, and G. Bisker, "Optical nanosensors for real-time feedback on insulin secretion by β-cells." *Small*, **17**, 2101660 (2021).
29. D. A. Heller, G. W. Pratt, J. Zhang, N. Nair, A. J. Hansborough, A. A. Boghossian, N. F. Reuel, P. W. Barone, and M. S. Strano, "Peptide secondary structure modulates single-walled carbon nanotube fluorescence as a chaperone sensor for nitroaromatics." *Proc. Natl Acad. Sci.*, **108**, 8544 (2011).
30. M. Zheng, A. Jagota, M. S. Strano, A. P. Santos, P. Barone, S. G. Chou, B. A. Diner, M. S. Dresselhaus, R. S. Mclean, and G. B. Onoa, "Structure-based carbon nanotube sorting by sequence-dependent DNA assembly." *Science*, **302**, 1545 (2003).
31. R. M. Williams, J. D. Harvey, J. Budhathoki-Uprety, and D. A. Heller, "Glutathione-S-transferase fusion protein nanosensor." *Nano Lett.*, **20**, 7287 (2020).
32. D. Roxbury, J. Mittal, and A. Jagota, "Molecular-basis of single-walled carbon nanotube recognition by single-stranded DNA." *Nano Lett.*, **12**, 1464 (2012).
33. D. Roxbury, X. Tu, M. Zheng, and A. Jagota, "Recognition ability of DNA for carbon nanotubes correlates with their binding affinity." *Langmuir*, **27**, 8282 (2011).
34. Z. Yaari, Y. Yang, E. Apfelbaum, C. Cupo, A. H. Settle, Q. Cullen, W. Cai, K. L. Roche, D. A. Levine, and M. Fleisher, "A perception-based nanosensor platform to detect cancer biomarkers." *Sci. Adv.*, **7**, eabj0852 (2021).
35. M. Kim, C. Chen, P. Wang, J. J. Mulvey, Y. Yang, C. Wun, M. Antman-Passig, H.-B. Luo, S. Cho, and K. Long-Roche, "Detection of ovarian cancer via the spectral fingerprinting of quantum-defect-modified carbon nanotubes in serum by machine learning." *Nat. Biomed. Eng.*, **6**, 267 (2022).
36. A. V. Naumov, S. Ghosh, D. A. Tsyboulski, S. M. Bachilo, and R. B. Weisman, "Analyzing absorption backgrounds in single-walled carbon nanotube spectra." *ACS nano*, **5**, 1639 (2011).
37. M. Itkis, D. Perea, S. Niyogi, S. Rickard, M. Hamon, H. Hu, B. Zhao, and R. Haddon, "Purity evaluation of as-prepared single-walled carbon nanotube soot by use of solution-phase near-IR spectroscopy." *Nano Lett.*, **3**, 309 (2003).
38. Y. Tan and D. E. Resasco, "Dispersion of single-walled carbon nanotubes of narrow diameter distribution." *J. Phys. Chem. B*, **109**, 14454 (2005).
39. N. Nair, M. L. Usrey, W.-J. Kim, R. D. Braatz, and M. S. Strano, "Estimation of the (n, m) concentration distribution of single-walled carbon nanotubes from photo-absorption spectra." *Anal. Chem.*, **78**, 7689 (2006).
40. H. Yu, W. J. Li, Y. Qu, X. Tian, Z. Dong, Y. Wang, K. Qin, and W. Ren, *2008 3rd IEEE International Conference on Nano/Micro Engineered and Molecular Systems* 540 Piscataway, NJ (IEEE).
41. J. A. Fagan, M. L. Becker, J. Chun, P. Nie, B. J. Bauer, J. R. Simpson, A. Hight-Walker, and E. K. Hobbie, "Centrifugal length separation of carbon nanotubes." *Langmuir*, **24**, 13880 (2008).
42. J. A. Fagan, J. Y. Huh, J. R. Simpson, J. L. Blackburn, J. M. Holt, B. A. Larsen, and A. R. H. Walker, "Separation of empty and water-filled single-wall carbon nanotubes." *ACS nano*, **5**, 3943 (2011).
43. J. Ackermann, J. T. Metternich, S. Herbertz, and S. Kruss, "Biosensing with fluorescent carbon nanotubes." *Angew. Chem. Int. Ed.*, **61**, e202112372 (2022).